RESEARCH PAPER

WATER QUALITY MONITORING USING MODELING OF SUSPENDED SEDIMENT ESTIMATION (A CASE STUDY: SEFIDROUD RIVER IN NORTHERN IRAN)

Mohammad Reza Salami[1], Ebrahim Fataei[*1], Fatemeh Nasehi[1], Behnam Khanizadeh[2], Hossein Saadati[1]

[1] Department of Environmental Sciences and Engineering,Ardabil Branch, Islamic Azad University, Ardabil, Iran

[2] Department of Chemistry, Sarab Branch, Islamic Azad University, Sarab, Iran

***Corresponding author:** Ebrahim Fataei, **Email:** eb.fataei@iau.ac.ir; eafataei@gmail.com

Received: October 28th 2024 / Accepted: November 22nd 2024 / Published: October 1st 2024

https://doi.org/10.24057/2071-9388-2024-3511

ABSTRACT. The Sefidroud River, the second largest river in Iran, is located in the north. Since the operation of the Sefidroud (Manjil) dam on the said river, about half of the storage volume of the dam has decreased as a result of the accumulation of sediments. The present research, using 516 suspended sediment data from four regional sediment monitoring stations, was conducted between 2013 and 2020 to check the accuracy of single-linear, bi-linear and middle-class sediment rating curves (SRCs) of four sediment monitoring stations as well as Landsat 8 images to estimate suspended sediment concentration (SSC). After drawing the SRCs based on 46 satellite images and SSC data, 70% of samples were used to prepare the regression models of spectral data versus suspended sediment discharge (Qs) and 30% of samples to evaluate the accuracy of SRC and Landsat 8 data. According to results, the middle-class SRCs had the highest coefficient of determination (R^2, exponential). Four band ratios B4/B3, B4/B2, B6/B5 and B7/B5 had exponential and power correlation with Qs, with the highest value for the band ratio B4/B3 (R^2 = 0.74, exponential). To conclude, the results of the current research showed that the B4/B3 band ratio was more efficient for Qs estimation.

KEYWORDS: Water pollution, suspended sediment discharge, Satellite Spectral Data ,Landsat 8

CITATION: Salami M. R., Fataei E., Nasehi F., Khanizadeh B., Saadati H. (2024). Water Quality monitoring Using Modeling of Suspended Sediment Estimation (A Case Study: Sefidroud River in Northern Iran). Geography, Environment, Sustainability, 4(17), 101-111

https://doi.org/10.24057/2071-9388-2024-3511

ACKNOWLEDGMENTS: This research is extracted from the dissertation of the Ph.D student (Mr. Mohammad Reza Salami) in Environmental Engineering and Science, Islamic Azad University of Ardabil Branch. Therefore, the authors appreciate the esteemed president, educational and research deputies of Ardabil Islamic Azad University for their cooperation in facilitating the implementation of this project.

Conflict of interests: The authors reported no potential conflict of interest.

INTRODUCTION

The water crisis, such as water scarcity, water pollution and other water-related issues, has been ranked fifth among the world's top 10 risks according to the Global Risk Report 2020 (Yang et al. 2022). Recent centuries have increasingly experienced various erosions and corresponding effects on surface water and soil at the local, national, continental and international policy levels. As a result, many studies have focused on soil erosion process, sediment dynamics, sediment assessment, reservoir sediment and environmental aspects of suspended sediment transport and subsequently special measures to reduce soil erosion (De Girolamo et al. 2015). Sediment transport and sedimentation lead to consequences such as the formation of sediment islands in the river course and as a result reducing the flood flow transfer capacity, reducing the lifespan of dams and storage capacity of reservoirs, corrosion of river structures and damage to water structures and fields, and sedimentation in the canal. The sediment load in rivers is mainly composed of suspended sediment load (SSL) and sediment bed load (SBL). The SSL consists of suspended particles transported due to river turbulence, and the SBL contains coarser particles that flow on the river bed. Suspended sediment concentration (SSC) is one of the main factors of disrupting the natural flow of water (Efthimiou 2019). Spatial and temporal changes of SSC are related to anthropogenic and natural factors (Sa'ad et al. 2021), so that population growth along with climate change leads to overexploitation of land, thus affecting the quantity and quality of water in dam reservoirs (Mazhar et al. 2022). The annual reduction in the storage capacity of dams in the world following the sedimentation is approximately 0.5 to 1% of the reservoir volume, which is more than 4 to 5% for many dams; therefore, most dams lose the main part of their water storage capacity within 25 to 30 years (Verstraeten et al. 2003). Suspended sediments are continuously transported and accumulated in a river system, thereby affecting river morphology and biological services (Martinez and Cox 2023; Jangjoo 2021). About 20 billion tons of suspended sediments enter the oceans annually because of erosion and transport of sediments in

river systems (Abbasi et al. 2021; Dos Santos et al. 2018). In general, suspended sediment accounts for 70-90% of the total annual river sediment (Pavanelli & Cavazza 2010; Regüés & Nadal-Romero 2013; Khan et al. 2021). In addition, suspended sediments, especially fine particles, are considered as physical pollutants due to the transport of chemicals (Safizadeh et al. 2021; Aires et al. 2022; Khoram Nejadian et al. 2023). Several studies reported a close relationship between SSC and heavy substances such as nitrate and phosphate (Endreny & Hassett 2005; Edwards and Withers 2008; Horowitz 2008; Cao et al. 2011; Wang et al. 2015).

In recent years, two methods of water sampling and the use of satellite spectrum have been employed to monitor the SSCs (Sa'ad et al. 2021). Water sampling is both time-consuming and more expensive (Sa'ad et al. 2021). In fact, the use of these conventional methods for water quality monitoring is challenging due to limited resources in terms of capital and available labor, especially in developing countries (Adjovu et al. 2023). On the other hand, SSC is very different in terms of time and space (Du et al. 2021), so that this natural heterogeneity makes it difficult to obtain a synoptic view of suspended sediments through in situ SSC sampling (Lei et al. 2021). Therefore, in recent years, indirect techniques, especially those that use satellite images, have become popular to investigate SSC in large rivers. These methods, which have been tested since early in the 21st century, are more cost- and time-effective (dos Santos et al. 2018). Sa'ad et al. (2021) in the east coast of Malaysia, by examining the statistical correlation of total suspended sediment (TSS) with Landsat 8 bands, concluded that TSS had a correlation coefficient (R^2) of 0.79 with the green, near-infrared (NIR), and short-wavelength (SWIR) bands. Jally et al. (2021) investigated the correlation of Landsat-8 Operational Land Imager (OLI) satellite data and SSC in Chilika Lake in eastern India and found that the multiband linear regression model ($R^2 = 0.6$) could explain SSC changes better than the single-band regression model ($R^2 = 0.39$). Cremon et al. (2020) used Top-of-Atmosphere (ToA) and Landsat 5 surface reflectance data in the Araguaia River in west-central Brazil, and showed that multiple regression models with ToA reflectance using VNIR bands, band ratios, SWIR band 5 could better explain SSC changes (adjusted $R^2 = 0.87$, normalized root mean square error (NRMSE) = 10.09%) compared to the models with surface reflectance (adjusted $R^2 = 0.6$, NRMSE = 15.43%). Wen et al. (2022) investigated the total suspended matter (TSM) of Chinese lakes using Landsat data and showed that the red band had a correlation with TSM ($R^2 = 0.76$). Aires et al. (2022) used the spectral data of Landsat 8 and Sentinel-2 satellites, and found a strong regression relationship between the NIR band of both satellites and surface sediment concentration. Martinez and Cox (2023) investigated SSC in the Middle-Mississippi and Lower-Missouri rivers in the United States using Landsat 8, 7, and 5 data, and reported that the R^2 value of the developed regression model was 0.72, 0.71 and 0.75 for the spectral reflectance of the mentioned satellites, respectively.

In addition to using single bands and band ratios for SSC monitoring, previous studies used satellite indices such as normalized difference water index (NDWI), normalized difference turbidity index (NDTI) and TSM to monitor water quality (Toming et al. 2017; Zhu et al. 2020; Meena et al. 2021; Das et al. 2021; Mazhar et al. 2022; Adjovu et al. 2023). Despite the fact that the majority of the aforementioned studies reported a high correlation coefficient for the regression models used, the efficiency of these regression models and their preference to SRCs are challenging and controversial. For this reason, in the present study, the effectiveness of Sediment rating curves (SRCs) and satellite spectral information to estimate of suspended sediment concentration (SSC). In an innovative approach at the same time and in a single location was analyzed and investigated. Accordingly, the present study aimed to estimate SSC in Sefidroud river in northern Iran using SRCs and satellite images and to validate the efficiency of the regression models of both methods using real field samples measured.

MATERIALS AND METHODS

Study area

The Sefidroud watershed is one of the largest watersheds in Iran and a subset of the Caspian Sea watershed, about 73% of which is located in the mountainous areas of the Alborz and Zagros mountain ranges and the rest in the plains and foothills (Othman et al. 2013). The area of this basin is 59,217 km^2 and its main river is Sefidroud (Ghaffari et al. 2022). As the second largest river in Iran, Sefidroud is formed by joining the Shahrood River (from the southeast side) and the Ghezel Ozan River (from the northeast side) near the city of Manjil (Khosravi et al. 2019) and is introduced to the Caspian Sea near Astaneh-ye Ashrafiyeh County after crossing the width of Gilan province. The mean annual discharge (MAD) of this river is 3998 million cubic meters. Manjil dam is located on Sefidroud in Manjil city, which was put into operation in 1963 with an initial storage capacity of 1.76 billion cubic meters at the normal level of the reservoir. This dam was built with the purpose of civil and economic development, flood control, organizing Sefidroud river, creating a suitable and reliable water source for supplying water to 24,000 hectares of agricultural lands in Gilan province and using hydroelectric potential energy (Othman et al. 2013). Climate changes and human interventions have greatly reduced the capacity of the lake behind this dam, so that reservoir siltation leads to the formation of a total of 32 million tons of sediment inside the lake every year; and now the volume of the reservoir has reached half of that during construction (the volume of the lake was 1.8 billion cubic meters at the time of construction and has reached 900 million cubic meters now) (Kavian et al. 2016). This study has used information from four regional sediment monitoring stations in Gilan. The Gilvan station is located on Ghezel Ozan River, the Lowshan station on Shahrood River, the Rudbar station on Sefidroud River after Manjil Dam, and the Astaneh-ye Ashrafiyeh station in Astaneh-ye Ashrafiyeh County near the shores of the Caspian Sea on the Sefidroud River. Fig. 1 shows the location of the studied stations.

Data analyzed in the study

The SSC of Sefidroud River water was monitored using data collected between 2013 and 2020 from four sediment monitoring stations of Gilvan, Lowshan, Rudbar and Astaneh-ye Ashrafiyeh affiliated to Gilan Regional Water Authority. At each station, the SSC and corresponding discharge data have been measured at least 10 times per year, so that a total of 122 data sets were recorded at Gilvan, 174 at Lowshan, 80 at Rudbar, and 140 at Astaneh-ye Ashrafiyeh stations during the eight-year period. After quality control for qualitative parameter data in terms of outliers, the SRCs were drawn for each of the stations based on eight years of data. The present research used the data of spectral bands of Level-1 Precision and Terrain (L1TP) Landsat 8 images. TP is the highest quality level-1 product suitable for pixel-level time series analysis (Sa'ad et al. 2021). To

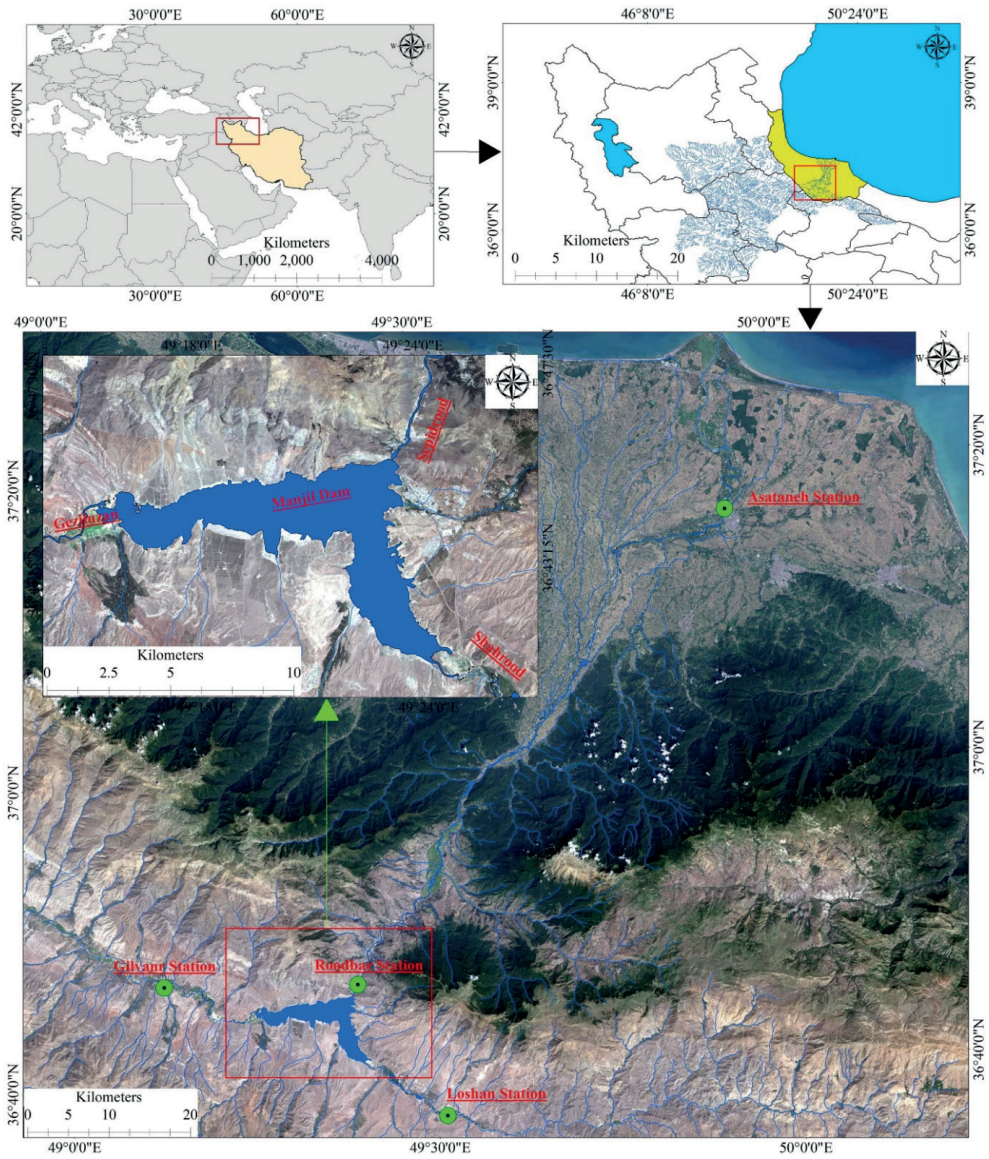

Fig. 1. Location of Sefidroud River and studied hydrometric stations, Gilan province, Iran

this end, 46 images captured by the Operational Land Imager (OLI; path: 166, row: 34) between 2013 and 2020 were acquired from the United States Geological Survey (USGS). The images were extracted at the same time as the SSC samples were taken (on the same day), and the criteria for selecting these images were based on the level of cloudiness and appropriate quality.

Drawing sediment rating curves

Normally, methods of sampling suspended sediment of water resources include interpolation and extrapolation procedures (Walling and Webb 1981, 1988; Walling 1994). The interpolation method assumes that the concentration or discharges obtained from the samples taken are representative of a long-term period (for example, days and weeks) and requires regular sampling. The extrapolation method estimates river sedimentation through more limited field measurements and establishing a relationship between the sediment discharge and the corresponding flow discharge; sediment rating curves (SRCs) are a typical example of the extrapolation method (Efthimiou 2019). the SRC method, the relationship between discharge and SSC is usually obtained according to Equation 1 (Asselman 2000; Efthimiou 2019; Khan et al. 2021; Azadi et al. 2020).

$$Q_s = \alpha Q_w^b \quad (1)$$

Where, Q_s stands for the sediment concentration or suspended sediment discharge in milligrams per liter (mgL^{-1}) or tones per day, Qw for the flow rate in cubic meters per second (m^3s^{-1}), and α and b for the constant coefficients of the regression equation.

The most common way to get the SRC is to pass a line through the point cloud of flow discharge and SSC, called single-linear SRC (Asselman, 2000; Azadi et al. 2020). Sometimes the distribution of point cloud is such that it needs to pass more than one line, which is called the broken line interpolation or bi-linear SRC (Zarris et al. 2011; Efthimiou 2019). In this method, first, the cumulative curve of SSC data versus flow discharge values is drawn in a log-polar coordinate system. Then, the amount of flow discharge at the point of abrupt change of slope and cumulative curvature is used as a base or initial guess for the separation of the data series (point cloud).

To draw bi-linear SRC, after drawing the graph of SSC cumulative curve and normal flow discharge data, the most suitable abrupt change point of SSC cumulative curve slope and the corresponding flow discharge was used as a base or initial guess to separate the data series (point cloud). In order to achieve the optimal flow discharge value of the data separator, different flow discharge values around the initial value were also tested by trial and error, and finally, the best result (flow discharge) was identified for the optimal separation of the initial series of data. Thus,

flow charges smaller and larger than 10, 45, 15 and 10 m3s-1 were used for Gilvan, Lowshan, Rudbar, and Astaneh-ye Ashrafiyeh stations, respectively, for data separation and bi-linear SRC drawing.

Jansson (1996) suggested that flow discharges should be divided into a number of classes with a certain trend, and for the mean discharge of each class, the mean SSC of the same group should be determined and the SRC should be drawn using these new data. This method is called middle-class SRC (Khaleghi & Varvani 2018). In order to determine the classes for drawing middle-class SRC, the discharge range smaller than 2 m^3/s for Gilvan and Lowshan stations, and the discharge range smaller than 5 $m^3s^{-1}$for Rudbar and Astaneh-ye Ashrafiyeh stations were considered as the first class. Then, the range of discharge changes in each class gradually increased, so that the range of changes of the last class of Gilvan, Lowshan, Rudbar and Astaneh-ye Ashrafiyeh stations was considered to be greater than 200, 130, 280 and 240 m^3s^{-1}, respectively. The reason is that the number of discharge episodes captured in larger discharges is limited. For example, the number of recorded episodes of the last class at Rudbar station (200 < m^3s^{-1}) was only 1, while the number of first-class episodes (5 > m^3s^{-1}) was 19. Therefore, 19, 18, 19 and 20 classes were determined for Gilvan, Lowshan, Rudbar and Astaneh-ye Ashrafiyeh stations, respectively, and middle-class SRC was drawn by calculating the mean SSC and flow discharge of each class.

Satellite image preprocessing

Remote sensing techniques to measure SSC use surface reflectance measured by multispectral sensors on satellites or cameras. Surface reflectance can be correlated with SSC to provide an indirect measure of SSC by creating SSC-surface reflectance models (Martinez and Cox 2023). in the present research, after receiving the mentioned satellite images, the data quality was controlled based on atmospheric, geometric and radiometric errors using ENVI 5.3 program. Since the majority of received images had a coordinate system, there was no need for geometric correction. One of the important challenges of remote sensing data in the investigation of water zones is the resolution and atmospheric correction of satellite images (Yang et al. 2022). Earth's atmosphere consists of liquid, solid and gas particles, many of which cause optical absorption, diffusion and scattering. The signal received by the satellite is emergent radiation from the earth's surface and atmosphere, which is recorded directly through the sensor. The radiation measured in the sensor is known as top of atmosphere (ToA). The purpose of atmospheric corrections is to convert the ToA radiation of objects into reflection from the Earth's surface. Therefore, the radiometric correction was first done by calibrating the digital numbers (DN) of the image to radiance (Cremon et al. 2020; Jally et al. 2021; Adjovu et al. 2023). Then, the atmospheric correction was performed using Fast Line-of-sight Atmospheric Analysis of Spectral Hypercubes (FLAASH) module. This module can correct wavelengths in the visible, NIR and SWIR regions up to 3 micrometers (Kantakumar and Neelamsetti 2015). The parameters required for the atmospheric correction were extracted from the MTL text file data as well as the Advanced Spaceborne Thermal Emission and Reflection Radiometer (ASTER) 30-meter DEM.

Fusion the images

Remote sensing studies are more interested in pixel-level image fusion (Xu and Ehlers 2017). Pixel-based satellite image fusion algorithms use the geometric details of a high-resolution panchromatic (PAN) image and spectral information from a multispectral (MS) image with low spatial resolution to generate a high spatial resolution MS image (Xu and Ehlers 2017; Pushparaj and Hegde 2017; Zhang et al. 2016). In recent years, many efforts have been made to provide algorithms suitable for fusion spectral and spatial information of satellite images (Kavzoglu and Colkesen 2009, Im et al. 2008, Yia et al. 2012; Liao et al. 2014). The current research used the Gram-Schmidt algorithm, in which a PAN band is simulated using the MS image spectral bands. Generally, in this algorithm, the simulated PAN band is obtained by averaging the MS image bands, and is considered as the first band. Then, the Gram-Schmidt transformation is conducted for the simulated PAN band and the MS bands. Next, the PAN band of the high-resolution image is replaced with the first Gram-Schmidt band (Sarp 2014; Pushparaj and Hegde 2017).

Correlation between spectral reflectance and suspended sediment concentration

After preliminary processing on satellite images, the correlation of SSC and spectral reflectance changes was analyzed. To this end, using random sampling in SPSS program, first 30% of the information of 46 satellite images and SSC (15 samples) were selected and left out of the data set; 70% of the data (spectral information of 31 satellite images) was used for the analysis of regression models, and the 30% left out was used in the stage of checking the efficiency of regression models of spectral information and SSC. It should be noted that in SPSS software, for random sampling of data, the percentage defined for sampling in the program environment is applied in a limited way. That is, to sample 30% of the data, the range of 25 to 35% of the data may be randomly sampled. For this reason, in the current research, about 30% defined in SPSS program, finally 33% (15 samples) and the rest (70%) finally 67% (31 samples) were sampled. In order to investigate the spectral reflectance of the runoff of Sefidroud, Ghezel Ozan and Shahrood rivers, first, five fixed 15-meter pixels were considered in all images from the location of the stations to 150 meters upstream of the station, followed by calculating the average values of spectral reflectance of seven image bands in these five pixels. It seemed that the average spectral reflectance of 5 fixed pixels at the closest point to the hydrometric stations compared to the spectral reflectance of one pixel was more suitable for SSC analysis due to the possibility of errors caused by the geometric and radiometric characteristics of the images. After extracting the spectral reflectance values of the image bands, the correlation between SSC and spectral reflectance of 7 bands and 21 band ratios was investigated. In such studies, the criterion is usually the ratio of the larger band to the smaller band. The band ratio B4/B3 is one of the most important spectral information in water pollution investigations, that is why this ratio is referred to as the TSM index, which is used in many studies to monitor water quality (Toming et al. 2017; Zhu et al. 2020; Das et al. 2021).

A total of 28 spectral parameters including bands and band ratios were used to check the correlation between qualitative parameters and spectral reflectance of the images. In choosing the most appropriate correlation equation in Excel, among the four regression equations, exponential, linear, logarithmic and power, the equation with higher correlation coefficients was selected as the best one.

Efficiency criteria of regression models

After analyzing SRCs and checking the correlation between SSC and 28 spectral reflectance parameters of 70% of the data, the models with the highest correlation coefficients were selected. Using the discharge values in the regression equations of SRCs and spectral reflectance, the SSCs were calculated in 30% of the left out data. Then, the estimated values from SRCs and satellite images were compared with the actual measured values. In order to evaluate the efficiency of the regression models, the percent error criterion was first used to get an overview of the error values of each of the correlation equations. For this purpose, first percent bias (PBIAS) was calculated according to Equation 2. The optimal value of this error is zero, and positive and negative values indicate overestimation and underestimation of the estimated data compared to the observed data, respectively (Jung et al. 2020). Its optimal value is zero and acceptable values are ±15% (Khan et al. 2021).

$$PBIAS = \frac{\sum_{i=1}^{n}\left(Qs_{obs} - Qs_{est}\right)}{\sum_{i=1}^{n} Qs_{obs}} \quad (2)$$

Where, Qs_{obs} is the sum of the observed SSC values in the desired period (30% of the total data), Qs_{est} is the sum of the estimated SSC values in the desired period (30% of the total data) and n is the number of observed and estimated data (equal to 15 in this research).

The estimated percent error provides an overview of the error values of each method, so other statistical criteria were also used to select the appropriate method. Thus, the statistical tests including mean absolute error (MAE), root mean square error (RMSE), Nash-Sutcliffe efficiency (NSE) and general standard deviation (GSD) were applied to evaluate, compare and validate each of the SRCs. These statistical criteria were calculated through Equations 3 to 6, respectively.

$$MAE = \frac{\sum_{i=1}^{n}\left|Qs_{obs} - Qs_{est}\right|}{N} \quad (3)$$

$$RMSE = = \sqrt{\frac{\sum_{i=1}^{n}\left(Qs_{obs} - Qs_{est}\right)^2}{N}} \quad (4)$$

$$NSE = 1 - \frac{\sum_{i=1}^{n}\left(Qs_{obs} - Qs_{est}\right)^2}{\sum_{i=1}^{n}\left(Qs_{obs} - \overline{Qs}_{obs}\right)^2} \quad (5)$$

$$GSD = \frac{RMSE}{\overline{Qs}_{est}} \quad (6)$$

Where, Qs_{obs} is the observed SSCs (in tons per day or mg/L), Qs_{est} is the estimated SSCs, and N is the number of observed samples.

The RMSE shows the distribution of the average difference between observed and estimated values, but it cannot provide information about overestimation and underestimation of the model (Farhadi et al. 2020; Ghadim et al. 2020). Like RMSE, the MAE is a common measure to show the average difference between observed and estimated values, but it is less sensitive to the output than RMSE, and one of its advantages is that it is preferred for smaller data sets (Efthimiou 2019). The NSE evaluates the residual variance of the estimated value compared to the variance of the measured data (Jung et al. 2020) and R2 describes the degree of collinearity among the observed and calculated data (Azadi et al. 2020). The value of NSE and R2 varies between zero and 1, and the higher the value, the lower the error, so that a value above 0.5 is acceptable for the model (Khan et al. 2021; Mackialeagha et al. 2022). The optimal equation was selected using the Simple Addition Ranking of the values of the evaluation indices. Thus, the closest values of MAE, NSE and R2 to the number 1 and the closest values of RMSE and GSD to the number zero in the desired station, which represents the smallest difference between the estimated and observed SSCs (Azadi et al. 2020; Ghadim et al. 2020; Adjovu et al. 2023), were assigned rank 1 and the next values were assigned rank 2. Then, the sum of the rank values of each method was compared to each other, and any method that had the lowest total rank was introduced as the optimal method. If the total ranks in two or more methods were equal, the priority was given to the equation of the method that had the highest R^2 value based on the correlation coefficient between the observed and estimated SSCs.

RESULTS

Drawing sediment rating curves

After quality control of sediment data measured at four sediment monitoring stations, a simple linear sediment curve was drawn for each station (Figure 2). The results showed that the R^2 value of the exponential correlation between SSC and the corresponding discharge in Gilvan, Lowshan, Rudbar and Astaneh-ye Ashrafiyeh stations was 0.67, 0.50, 0.79 and 0.81, respectively. The fitted line of exponential regression also revealed that suspended sediment discharge (Q_s) started from lower water discharges (Q_w) in Gilvan, Lowshan and Astaneh-ye Ashrafiyeh stations, but Astaneh-ye Ashrafiyeh station had lower Q_s compared to Gilvan and Lowshan stations, per corresponding water discharge (Q_w), while in Rudbar station, compared to Gilvan, Lowshan, and Astaneh-ye Ashrafiyeh stations, Q_w for Q_s initiation was more, and compared to Astaneh-ye Ashrafiyeh station, Q_s was more for Q_w.

Fig. 3 shows bi-linear SRCs drawn for the studied stations. The results indicated that, apart from Rudbar station, the R^2 value of at least one of the regression equations increased in three other stations. The R^2 value was 0.31, 0.56, 0.06 and 0.73 for the discharges lower than Astaneh-ye Ashrafiyeh station and 0.64, 0.12, 0.43 and 0.30 for the discharges higher than Astaneh-ye Ashrafiyeh station at Gilvan, Lowshan, Rudbar and Astaneh-ye Ashrafiyeh stations, respectively.

Fig. 4 shows middle-class SRCs drawn for the studied stations. The results showed that the R^2 value of middle-class SRCs in all four studied stations was higher than that of both single-linear and bi-linear SRCs, so that it was 0.85, 0.65, 0.56 and 0.83 for Gilvan, Lowshan, Rudbar and Astaneh-ye Ashrafiyeh stations, respectively. These results indicated that middle-class SRCs were more accurate in predicting flow discharge and SSC values compared to single-linear and bi-linear SRCs due to the highest value of R^2.

The results obtained from the regression models of suspended sediment concentration and spectral bands

The results showed that among 28 spectral parameters (including 7 bands and 21 band ratios), four band ratios B4/B3, B4/2, B6/B5 and B7/B5 had an exponential and power correlation with the R^2>0.35 (Fig. 4). The R^2 value of band ratios B4/B3 and B4/2 with exponential and power correlation was 0.74 and 0.43, respectively, and the R^2 value of band ratios B6/B5 and B7/B5 with exponential correlation was 0.46 and 0.39, respectively. The band ratios B4/B3 and B4/2 had a direct relationship with Q_s, so that the increase in the values of these band ratios was accompanied by the increase in Q_s, but the relationship of band ratios B6/B5 and B7/B5 with Q_s was inverse, so that the increase of these ratios was associated with the decrease of Q_s.

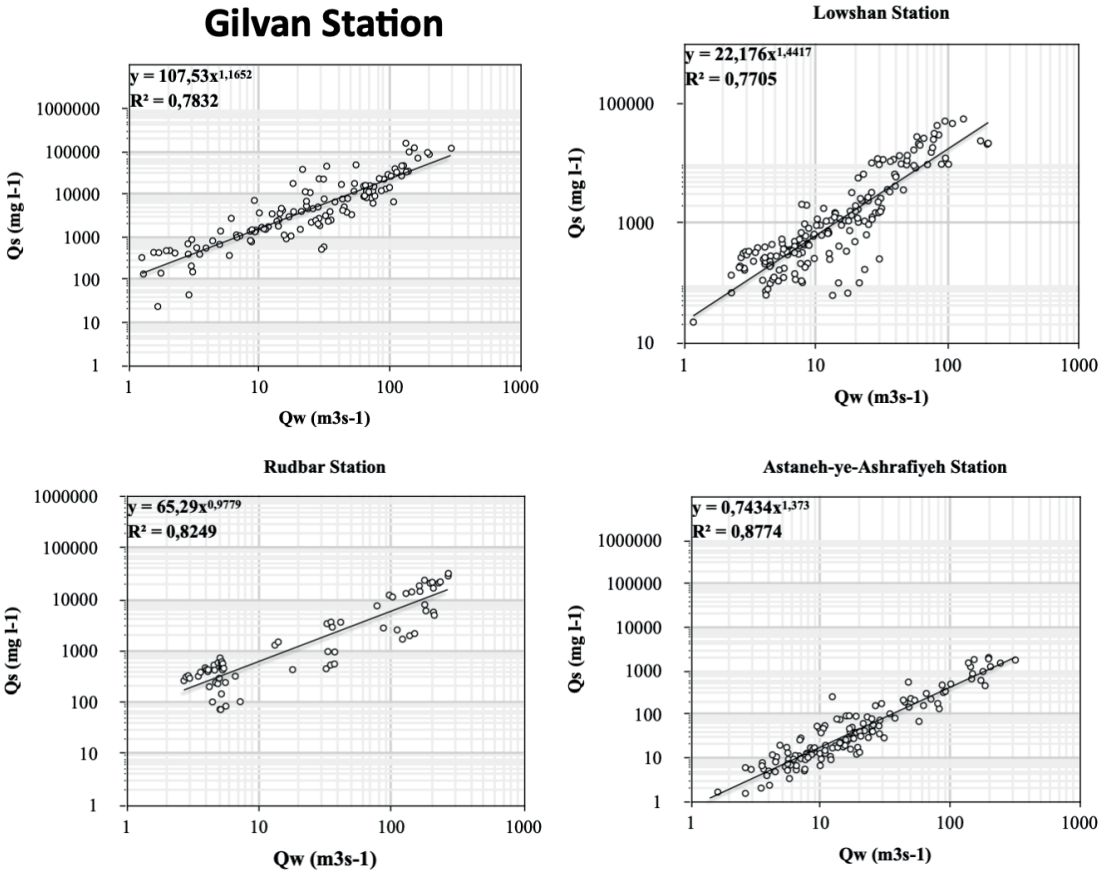

Fig. 2. Single-linear sediment rating curves drawn for the studied stations

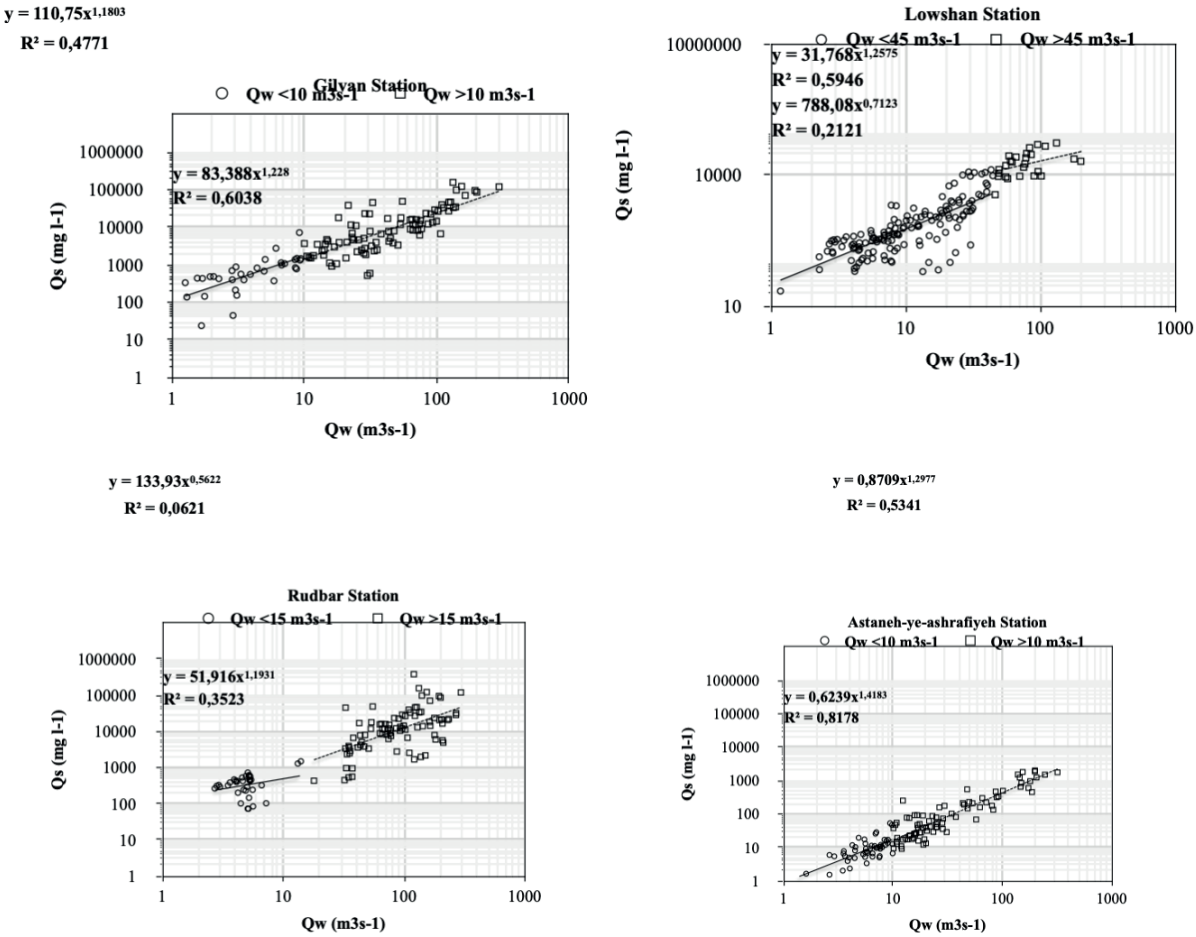

Fig. 3. Bi-linear sediment rating curves drawn for the studied stations

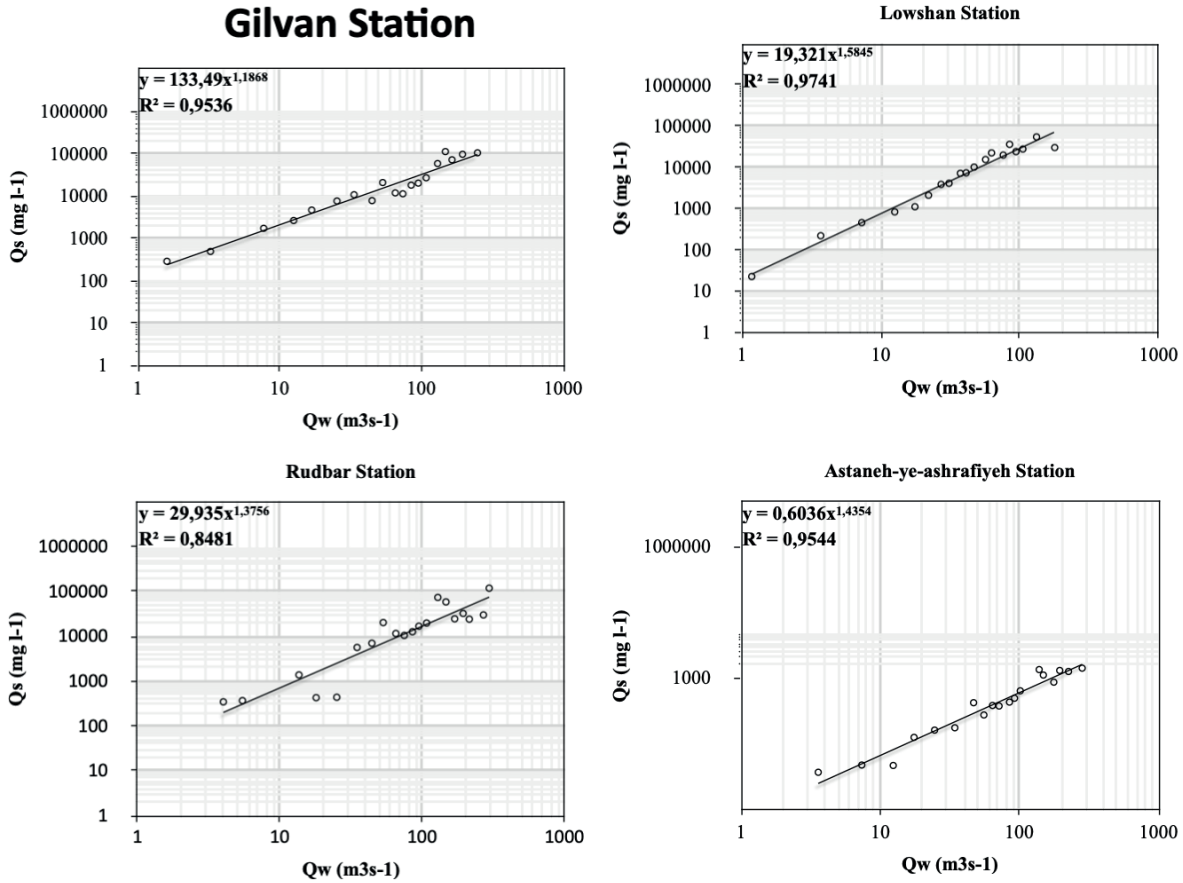

Fig. 4. Middle-class sediment rating curves drawn for the studied stations

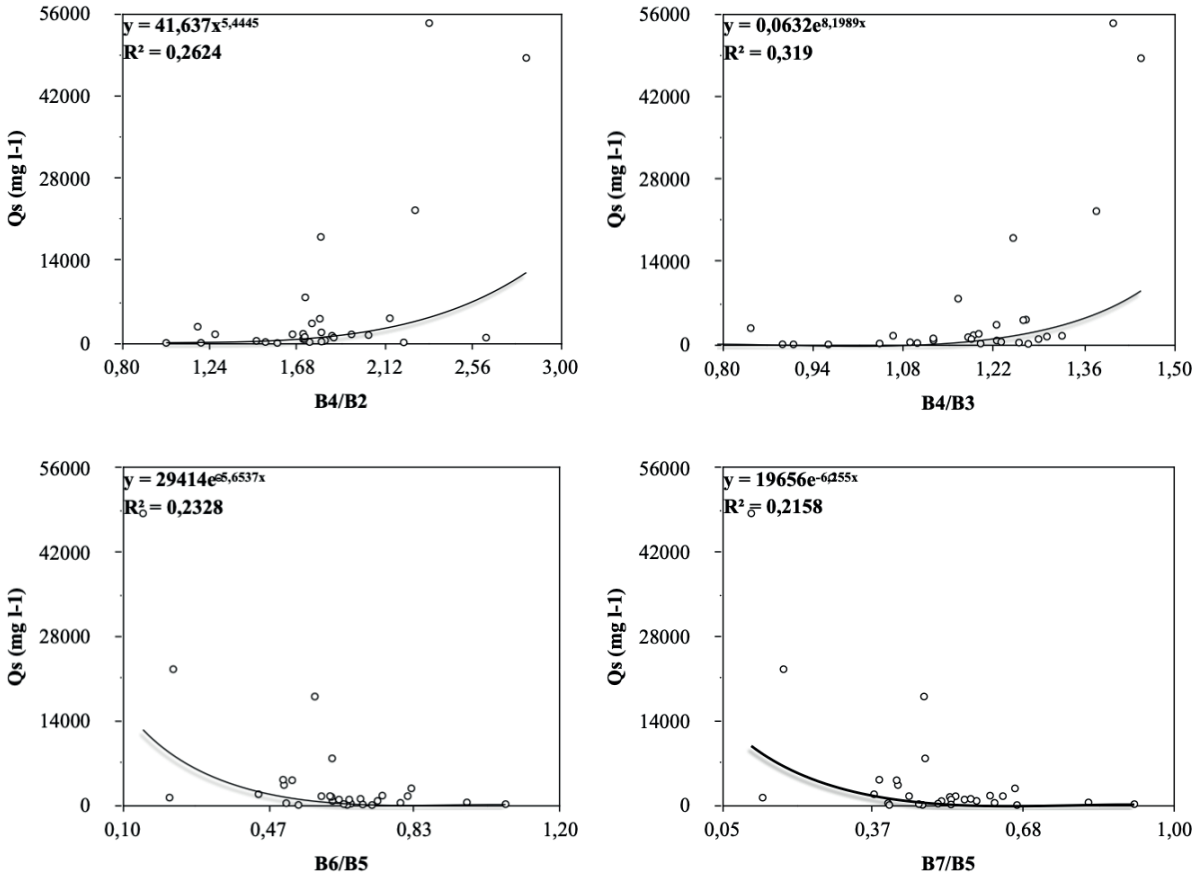

Fig. 5. Regression model of satellite spectral bands versus suspended sediment discharge (Q_s)

Determining the efficiency of regression models

The results revealed that the middle-class SRCs in the three stations of Gilvan, Lowshan and Astaneh-ye Ashrafiyeh had higher R^2 values. In addition, at Rudbar station, single-linear SRC had the highest R^2 value. Among the regression relationships of Q_s versus satellite band ratios, the B4/B3 band ratio had the highest R2 value. Therefore, to check the efficiency of the mentioned regression models, the values of the statistical criteria were calculated using 30% of the data (15 samples) (Table 1). The results showed that the regression equation B4/B3 versus Q_s was underestimated and the SRC equations were overestimated, so based on the PBIAS index, using the B4/B3 band ratio, the total Q_s in 15 samples was underestimated by about 51%, while using SRCs, the total Q_s was estimated to be around 15% more. However, the Q_s values estimated from B4/B3 band ratio had lower MAE, RMSE and NSE (2723 and 6055 mg/L and 46%, respectively), while the Qs values estimated from SRCs had higher MAE, RMSE and NSE (4198, 9125 mg/L and 22%, respectively). In addition to lower PBIAS, the Q_s values estimated from SRCs also had lower GSM (2.24). However, considering the impact of all efficiency criteria on the accuracy of regression models, the ranking of error values and total rankings showed that Q_s values estimated from B4/B3 band ratio with a total rank of 7 compared to Q_s values estimated from SRCs with a total rank of 8 were in the first priority (Table 2).

Investigating the regression relationship of Q_s values estimated from the band ratio B4/B3 and SRCs with the observed values of Q_s based on four exponential, linear, logarithmic and power correlation equations showed that the values of Q_s estimated from the band ratio B4/B3 had an exponential relationship and the values of Q_s estimated from SRCs had a logarithmic relationship. The findings of the present study indicated that the R2 value of the Q_s estimated from the band ratio B4/B3 was much higher compared to the Q_s estimated from SRCs (86% versus 14%). Therefore, both the total ranking of the efficiency criteria of the regression model and R_2 of the estimated to observed Q_s values showed that the regression equation of band ratio B4/B3 had better efficiency for Q_s estimation.

DISCUSSION AND CONCLUSION

Sediment concentration (SSC)

During the period of 2013 to 2020, the present study monitored suspended sediment concentration (SSC) using single-linear, bi-linear and middle-class sediment rating curves (SRCs) as well as Landsat 8 images in four sediment monitoring stations on Sefidroud river in northern Iran. The results indicated that the middle-class SRCs predominantly had higher coefficient of determination (R_2, exponential) at all stations. The middle-class SRCs were invented by Jansson (1996) in a study of the Reventzon river basin in Costa Rica by sampling and using the data of the Palomo sediment monitoring station to reduce the logarithmic retransformation bias of the single linear sediment rating curve. The results of Jansson (1996) showed that the estimate of sediment concentration using middle-class SRC was very close to the observed values, while single-linear SRC showed a lower estimate. One of the important advantages of using middle-class SRC can be neutralizing the effect of having more samples in low discharges in the calendar statistics method; because by averaging the data in flow classes, the large number of observations in the base discharges will no longer have an effect on the

Table 1. Efficiency criteria of regression models of sediment rating curves and B4/B3 band ratio based on suspended sediment discharge

Regression model	PBIAS	MAE	RMSE	NSE	GSD
Sediment rating curves	14.51	4197.95	9125.25	-0.22	2.24
Band ratio B4/B3	-51.48	2722.96	6054.81	0.46	3.51

Table 2. Ranking of efficiency criteria and priority of regression models of sediment rating curves and B4/B3 band ratio based on suspended sediment discharge

Regression model	PBIAS	MAE	RMSE	NSE	GSD	Total ranks	Priority
Sediment rating curves	1	2	2	2	1	8	2
Band ratio B4/B3	2	1	1	1	2	7	1

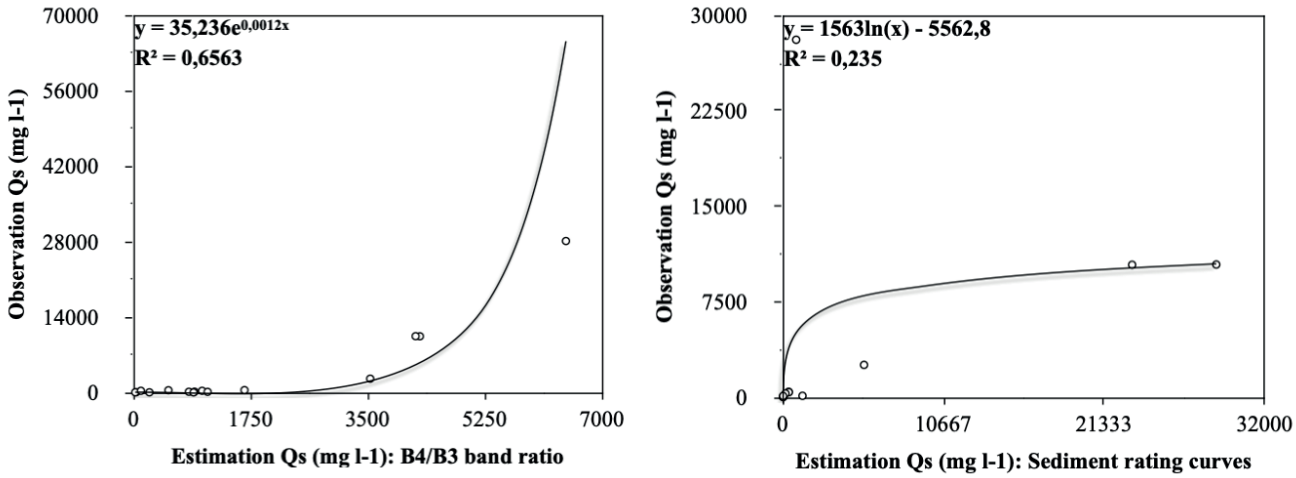

Fig. 6. The regression relationship of suspended sediment discharge estimated from the band ratio B4/B3 and sediment rating curves with observed suspended sediment discharge

SRC. Walling and Webb (1981 and 1988) and Walling (1994) suggested that the quality of the SRC can be improved by giving more weight to higher discharges that have higher sediment concentrations. Accordingly, in middle-class SRCs, due to the reduction of the effect of low points, the estimation of sediment in high discharges is improved, and also in this method, the distribution of points is reduced and the error caused by logarithmic transformation is minimized. On the other hand, the results related to the bilinear SRC indicated that in three of the four studied sediment monitoring stations, the R2 value of at least one of the bilinear regression equations increased compared to the single linear one. These results are consistent with the findings of Efthimiou (2019) and Zarris (2019), so that Efthimiou (2019) in a research on the suspended sediments of the Venetikos River in northern Greece and Zarris (2019) in the Nestos River on the border between Greece and Bulgaria showed that the bi-linear SRC had better efficiency for estimating SSC than the single linear one.

Spectral reflectance

The results of investigating the correlation between SSC and spectral reflectance of 7 single bands and 21 band ratios, 31 Landsat 8 satellite images, showed that four band ratios B4/B3, B4/2, B6/B5 and B7/B5 had exponential and power correlations with Q_s so that the band ratio B4/B3 (R^2= 0.74, exponential) had the highest correlation with Q_s. In the studies related to the relationship between satellite spectral information and suspended sediment, many researchers have focused on the green (B3: Green), red (B4: Red), near infrared (B5: NIR) and short wave infrared (B7 and B6: SWIR) bands. Sa'ad et al. (2021) found the R^2 value of 79% between the TSS and the green, near-infrared and short-wave infrared spectral bands of Landsat 8 on the east coast of Malaysia. Jally et al. (2021) also obtained 60% correlation between Landsat 8 spectral bands in Chilika Lake in eastern India. Cremon et al. (2020) improved the correlation coefficient of near-infrared and short-wave infrared bands and band ratios of Landsat 5 with SSC to about 87% in the Araguaia River in west-central Brazil. Wen et al. (2022) also showed in Chinese lakes that Landsat red band had a correlation coefficient of 0.76 with TSM. Aires et al. (2022) also reported a strong regression relationship between the NIR band of both Landsat 8 and Sentinel-2 satellites and suspended sediments. Martinez and Cox (2023) showed the correlation of Landsat 8, 7 and 5 spectral bands with SSC (R^2 = 0.72, 0.71 and 0.75, respectively) in the Mississippi and Missouri rivers in the United States of America.

The results related to the investigation of SRC efficiency and regression model between band ratio B4/B3 and Q_s using 15 measured land samples showed that although the SRCs compared to the regression model between the band ratio B4/B3 and Q_s had lower errors of PBIAS (15 versus -51%) and GSM (3.5 versus 2.2), the regression model between the band ratio B4/B3 and Q_s with lower MAE, RMSE and NSE errors (2723 and 6055 mg/L and 46% respectively) compared to SRCs (4198, 9125 mg/liter and 22%, respectively) was able to better estimate Q_s values in general. , the ranking of the overall efficiency criteria is actually the ranking of the validation criteria used in the current research. Any validation criterion that has more accuracy has been assigned a lower rank, and finally, any method with a lower numerical value has been selected as a more efficient method. In this research, the results showed that the band ratio B4/B3 has a lower rank.

In addition, the correlation coefficient between the estimated and observed Q_s showed that the Q_s estimated from the band ratio B4/B3 with the exponential regression model had a much higher R^2 (86% versus 24%) compared to the Q_s estimated from the SRC. This result is in line with the findings of Zhu et al. (2020), as the aforementioned researchers also investigated the regression relationship between Qs values observed and estimated from the B4/B3 band ratio of Landsat 8 in West Lake, Zhejiang Province, China, and came to the conclusion that there was an exponential relationship (R^2=82%) between the observed and estimated values.

In general, the results of the present study showed that satellite spectral information, especially the B4/B3 band ratio, had a very favorable capability for estimating suspended sediments. Considering that recording SSC data in sediment monitoring stations requires manpower and laboratory work, and in addition, more time is spent on sampling, laboratory work, and setting sediment data, free access to satellite images can effectively reduce costs and save time. On the other hand, sample collection in sediment monitoring stations is in the form of point and in situ sampling, while SSC varies according to the conditions of the river, in different regions and during different intervals (Du et al. 2021). Therefore, it is impossible to monitor the spatial changes of SSC along the river or water zones using SRCs (Lei et al. 2021), because it is impossible to sample all water zones due to financial and time constraints, and in some cases, easy access to all points is impossible due to the topographical conditions of the rivers and water areas. Meanwhile, one of the advantages of satellite images, regardless of its accuracy in estimating suspended sediments, is that satellite data captures ground information in a raster form in a wide area at the same time. Therefore, access to this raster information with spectral value and applying regression models on the spectral information of that zone easily provides the possibility of monitoring the spatial changes of phenomena, including water pollution, in all zones, even areas with difficult access. This helps water resource managers and decision makers to prepare a map of water pollution changes along the watershed and identify critical areas of water pollution and its causes in order to make appropriate decisions.

REFERENCES

Abbasi A, Taghavi L, Sarai Tabrizi M (2021) Qualitative Zoning of Groundwater to Assessment Suitable Drinking Water Using GIS Software in Mohammad Shahr, Meshkinshahr, and Mahdasht in Alborz Province. Anthropogenic Pollution. doi: 10.22034/ap.2021.1907787.1076

Adjovu GE, Stephen H, James D, Ahmad S (2023) Overview of the Application of Remote Sensing in Effective Monitoring of Water Quality Parameters. Remote Sensing 15(7):1938

Aires URV, da Silva DD, Fernandes Filho EI, Rodrigues LN, Uliana EM, Amorim RSS, de Melo Ribeiro CB, Campos JA (2022) Modeling of surface sediment concentration in the Doce River basin using satellite remote sensing. Journal of Environmental Management 323:116207

Asselman NEM (2000) Fitting and interpretation of sediment rating curves. Journal of hydrology 234(3-4):228-248

Cao Z, Zhang X, Ai N (2011) Effect of sediment on concentration of dissolved phosphorus in the Three Gorges Reservoir. International Journal of Sediment Research 26(1):87-95

Cremon ÉH, da Silva AMS, Montanher OC (2020) Estimating the suspended sediment concentration from TM/Landsat-5 images for the Araguaia River–Brazil. Remote Sensing Letters 11(1):47-56

Das S, Kaur S, Jutla A (2021) Earth observations-based assessment of impact of COVID-19 lockdown on surface water Quality of Buddha Nala, Punjab, India. Water 13(10):1363

De Girolamo AM, Pappagallo G, Lo Porto A (2015) Temporal variability of suspended sediment transport and rating curves in a Mediterranean river basin: The Celone (SE Italy). CATENA 128:135-143

dos Santos ALMR, Martinez JM, Filizola Jr NP, Armijos E, Alves LGS (2018) Purus River suspended sediment variability and contributions to the Amazon River from satellite data (2000–2015). Comptes Rendus Geoscience 350(1-2):13-19

Du Y, Song K, Liu G, Wen Z, Fang C, Shang Y, Zhao F, Wang Q, Du J, Zhang B (2020) Quantifying total suspended matter (TSM) in waters using Landsat images during 1984–2018 across the Songnen Plain, Northeast China. Journal of environmental management, 262:110334

Edwards AC, Withers PJA (2008) Transport and delivery of suspended solids, nitrogen and phosphorus from various sources to freshwaters in the UK. Journal of Hydrology 350(3–4):144-153

Efthimiou N (2019) The role of sediment rating curve development methodology on river load modeling. Environmental monitoring and assessment 191:1-19

Endreny Th, Hassett J (2005) Robustness of pollutant loading estimators for sample size reduction in a suburban watershed. Intl. J. River Basin Manage, (IAHR & INBO) 3(1):53-66

Farhadi H, Fataei E, Kharrat Sadeghi M (2020) The Relationship Between Nitrate Distribution in Groundwater and Agricultural Landuse (Case study: Ardabil Plain, Iran). Anthropogenic Pollution. doi: 10.22034/ap.2020.1885788.1059

Ghadim HB, Salarijazi M, Ahmadianfar I, Heydari M, Zhang T (2020) Developing a Sediment Rating Curve Model Using the Curve Slope. Polish Journal of Environmental Studies 29(2):1151–1159

Ghaffari A, Nasseri M, Pasebani Someeh A (2022) Assessing the economic effects of drought using Positive Mathematical Planning model under climate change scenarios. Heliyon 8:e11941

Horowitz AJ (2008) Determining annual suspended sediment and sediment-associated trace element and nutrient fluxes. Science of The Total Environment 400(1–3):315-343

Im J Jensen, Tullis J (2008) Object-based change detection using correlation image analysis and image segmentation, International Journal of Remote Sensing 29:399-423

Jangjoo MR (2021). Modelling fuzzy multi-criteria decision-making method to locate industrial estates based on geographic information system. Anthropogenic Pollution. doi: 10.22034/ap.2021.1933630.1111

Jally SK, Mishra AK, Balabantaray S (2021) Retrieval of suspended sediment concentration of the Chilika Lake, India using Landsat-8 OLI satellite data. Environmental Earth Sciences 80:1-18

Jansson MB (1996) Estimating a sediment rating curves of the Reventzon river at Palomo using logged mean loads within discharge classes, Journal of Hydrology, 183(4):227-241

Jung BM, Fernandes EH, Möller Jr OO, García-Rodríguez F (2020) Estimating suspended sediment concentrations from flow discharge data for reconstructing gaps of information of long-term variability studies. Water 12(9):2382

Kavian A, Dodangeh S, Abdollahi Z (2016) Annual suspended sediment concentration frequency analysis in Sefidroud basin, Iran. Modeling Earth Systems and Environment 2:1-10

Kavzoglu T, Colkesen I (2009) A Kernel function analysis for support vector machines for land cover classification. International Journal of Applied earth observation and Geoinformation 11:352-359

Khaleghi MR Varvani J (2018) Sediment rating curve parameters relationship with watershed characteristics in the semiarid river watersheds. Arabian Journal for Science and Engineering 43(7):3725-3737

Khan MA, Stamm J, Haider S (2021) Assessment of soft computing techniques for the prediction of suspended sediment loads in rivers. Applied Sciences 11(18):8290

khoram nejadian S, Esmaili A, Asemi S, Shams-Esfandabad B (2023) Determining heavy metal and developing model for concentration in the feathers of house sparrow (Ni, Pb,Cd) in Tehran. Anthropogenic Pollution. doi: 10.22034/ap.2023.1983320.1154

Khosravi K, Rostaminejad M, Cooper JR, Mao L, Melesse AM (2019) Dam break analysis and flood inundation mapping: The case study of Sefid-Roud Dam, Iran. In Extreme hydrology and climate variability 395-405

Lei S, Xu J, Li Y, Li L, Lyu H, Liu G, Chen Y, Lu C, Tian C, Jiao W (2021) A semi-analytical algorithm for deriving the particle size distribution slope of turbid inland water based on OLCI data: A case study in Lake Hongze. Environmental Pollution 270:116288

Liao K, Xu S, Wu J, Zhu Q, An L (2014) Using support vector machines to predict cation exchange capacity of different soil horizons in Qingdao City, China. J. Plant Nutrition Soil Science 177(5):775-782

Mackialeagha M, Salarian MB, Behbahaninia A (2022) The use of multivariate statistical methods for the classification of groundwater quality: a case study of aqueducts in the east of Tehran, Iran. Anthropogenic Pollution. doi: 10.22034/ap.2022.1965587.1134

Martinez MJ, Cox AL (2023) Remote-Sensing Method for Monitoring Suspended-Sediment Concentration on the Middle-Mississippi and Lower-Missouri Rivers. Journal of Contemporary Water Research & Education 177(1):17-30

Mazhar N, Javid K, Akram MAN, Afzal A, Hamayon K, Ahmad A (2023) Index-Based Spatiotemporal Assesment of Water Quality in Tarbela Reservoir, Pakistan (1990– 2020). Geography, Environment, Sustainability 15(4):232-242

Meena SR, Chauhan A, Bhuyan K, Singh RP (2021) Chamoli disaster: pronounced changes in water quality and flood plains using Sentinel data. Environmental earth sciences 80(17):601

Othman F, Sadeghian MS, Ebrahimi F, Heydari M (2013) A study on sedimentation in sefidroud dam by using depth evaluation and comparing the results with USBR and FAO methods. Int. Proc. Chem. Biol. Environ. Eng 51(9):6

Pavanelli D, Cavazza C (2010) River suspended sediment control through riparian vegetation: a method to detect the functionality of riparian vegetation. Clean Soil Air Water 38(11):1039-1046

Pushparaj J, Hegde AV (2017) Evaluation of pan-sharpening methods for spatial and spectral quality. Applied Geomatics:9(1):1-12

Regüés D, Nadal-Romero E (2013) Uncertainty in the evaluation of sediment yield from badland areas: Suspended sediment transport estimated in the Araguás catchment (central Spanish Pyrenees). CATENA 106:93-100

Sa'ad FNA, Tahir MS, Jemily NHB, Ahmad A, Amin ARM (2021) Monitoring total suspended sediment concentration in spatiotemporal domain over Teluk Lipat utilizing Landsat 8 (OLI). Applied Sciences 11(15):7082

Safizadeh E, Karimi D, Gahfarzadeh HR, Pourhashemi SA (2021) Investigation of physicochemical properties of water in downstream areas of selected dams in Aras catchment and water quality assessment (Case study: Aras catchment in the border area of Iran and Armenia). Anthropogenic Pollution. doi: 10.22034/ap.2021.1912491.1082

Sarp G (2014) Spectral and spatial quality analysis of pan-sharpening algorithms: A case study in Istanbul. European Journal of Remote Sensing 47(1):19-28

Toming K, Kutser T, Uiboupin R, Arikas A, Vahter K, Paavel B (2017) Mapping water quality parameters with sentinel-3 ocean and land colour instrument imagery in the Baltic Sea. Remote Sensing 9(10):1070

Verstraeten GJ, Poesen JDV, Koninckx X (2003) Sediment yield variability in Spain: a quantitative and semiqualitative analysis using reservoir sedimentation rates. Geomorphology 50(4): 327-348

Walling DE, Webb BW (1988) The reliability of rating curve estimates of suspended sediment yield: some further comments. In: Proceedings of the Porto Alegre Symposium BSediment budgets, 11–15 December, Porto Alegre, Brazil. IAHS Publication 174:337–350. Wallingford, UK: IAHS Press.

Walling DE, Webb BW (1988) The reliability of rating curve estimates of suspended sediment yield: Some further comments, In Sediment Budgets. Proc. Of Porto Symp. Dec. 1988, IAHS Publ, (174): 337 - 350.

Walling DE (1994) Measuring sediment yield from river basins, in: R. Lal (Edd), Soil erosion Research Methods. Soil and Water Conservation Society pobl, 2nd eddition: 39-83

Wang X, Liu Z, Miao J, Zuo N (2015) Relationship between nutrient pollutants and suspended sediments in upper reaches of Yangtze River. Water Science and Engineering 8(2):121-126

Wen Z, Wang Q, Liu G, Jacinthe PA, Wang X, Lyu L, Tao H, Ma Y, Duan H, Shang Y, Zhang B (2022) Remote sensing of total suspended matter concentration in lakes across China using Landsat images and Google Earth Engine. ISPRS Journal of Photogrammetry and Remote Sensing 187:61-78

Xu S, Ehlers M (2017) HYPERSPECTRAL IMAGE SHARPENING BASED ON EHLERS FUSION. International Archives of the Photogrammetry, Remote Sensing and Spatial Information Sciences, XLII-2/W7: 941-947

Yang H, Kong J, Hu H, Du Y, Gao M, Chen F (2022) A review of remote sensing for water quality retrieval: progress and challenges. Remote Sensing 14(8):1770

Yia L, Binga L, Qian-lia L, Chenc P, Yuana L (2012) A Change Detection Method for Remote Sensing Image Based on Multi-Feature Differencing Kernel Svm,» ISPRS Annals of Photogrammetry, Remote Sensing and Spatial Information Sciences 1:227-235

Zarris D, Vlastara M, Panagoulia D (2011) Sediment Delivery Assessment for a Transboundary Mediterranean Catchment: The Example of Nestos River Catchment. Water Resources Management 25(14):3785-3803

Zhang J, Yang J, Reinartz P (2016) The optimized block-regression-based fusion algorithm for pan sharpening of very high-resolution satellite imagery. The International Archives of the Photogrammetry, Remote Sensing and Spatial Information Sciences, Volume XLI-B7, 2016 XXIII ISPRS Congress, 12–19 July 2016, Prague, Czech Republic.

Zhu W, Huang L, Sun N, Chen J, Pang S (2020) Landsat 8-observed water quality and its coupled environmental factors for urban scenery lakes: A case study of West Lake. Water Environment Research 92(2):255-265